

Supporting Information

Monolayer-Protected Nanoparticle Doped Xerogels as Functional Components of Amperometric Glucose Biosensors

Michael H. Freeman, Jackson R. Hall, and Michael C. Leopold*

*Department of Chemistry, Gottwald Center for the Sciences, University of Richmond
Richmond, VA 23173*

Contents:

- ▶ Additional experimental details of procedures for the synthesis and characterization of MPCs, xerogels and MPC-doped xerogels.
- ▶ Additional SEM characterization of xerogels with and without MPC doping (Effects of humidity during drying/storage on sol-gel structure – including humidity-controlled chamber apparatus)
- ▶ Additional TEM characterization of xerogels with and without MPC doping, including cross-sectional TEM imaging
- ▶ Additional voltammetry of redox probes (ruthenium hexaamine and potassium ferricyanide) at various stages of xerogel sensor assembly
- ▶ Long term (45 day) stability data for sensor sensitivity and response time.
- ▶ Representative *I-t* curves for GOx embedded MPTMS xerogels doped with C6-MPCs – typical interferent responses
- ▶ Effects of variable xerogel drying times and humidity on glucose *I-t* and calibration curves
- ▶ Representative amperometric *I-t* curves, response time analysis, and stability monitoring of xerogel modified electrodes with and without MPCs generating the “low current” response typically achieved when shorter (≤ 2 hours) sol-gel drying times at 50-60% relative humidity are employed
- ▶ Representative *I-t* curves for GOx embedded MPTMS xerogels doped with C6-MPCs illustrating sol-gel deposition mixture dependence
- ▶ Table of comparison for analytical performance of glucose biosensors with and without incorporated nanoparticles from the literature

* To whom correspondence should be addressed. Email: mleopold@richmond.edu.
Phone: (804) 287-6329. Fax: (804) 287-1897.

Additional Experimental Details/Procedures:

MPC Synthesis

Alkanethiolate-protected MPCs were synthesized via minor modifications to the well-known Brust reaction regularly performed in our laboratory and others.³⁹⁻⁴⁰ Briefly, an aqueous solution of $\text{HAuCl}_4 \cdot 3\text{H}_2\text{O}$ (0.31 g in ~25 mL) was added to a toluene solution of tetraoctylammonium bromide (~1.1 g in ~30 mL toluene) to facilitate phase transfer of the gold to the nonaqueous layer. Hexanethiol or dodecanethiol was added in a 2:1 ratio to the separated non-aqueous gold-containing phase and allowed to stir for 30 minutes until the solution is a pale yellow color. This pale-yellow solution is subsequently placed on ice for 30 minutes to chill to $\sim 0^\circ\text{C}$. Chilled ($\sim 0^\circ\text{C}$), aqueous NaBH_4 solution (0.38 g in 20 mL) is then steadily poured into the mixture over a course of ~ 2 minutes to reduce the gold in the presence of the thiol ligands. This reaction is allowed to stir overnight and is rotary evaporated to near complete dryness. Precipitation and isolation of the MPCs is induced by the addition of 200 mL of acetonitrile and subsequent filtration through a medium glass-fritted funnel (ChemGlass). As in previous work,²⁹⁻³³ MPC diameter was assessed with TEM imaging and ligand structure and coverage was verified through NMR spectroscopy of *d*-methylene chloride solutions of MPCs. The average structure of the MPCs used in this study is $\text{Au}_{225}(\text{C}6)_{75}$ and is consistent with prior work in this lab and others.²⁹⁻³³ For certain experiments, MPCs were subsequently modified with 11-mercaptoundecanoic acid (MUA) using well-established place-exchanged reactions described in detail elsewhere.³⁰⁻³¹

For general TEM characterization of MPCs after synthesis, toluene solutions of MPCs were drop-coated onto Formvar carbon grids (Electron Microscopy Sciences) prior to imaging (JEOL 1010 TEM). The average diameter of the MPCs was approximately 2.0 (± 0.8) nm and consistent with all of our prior work with these materials.³¹⁻³³

Microscopy Characterization of Materials

For general TEM characterization of MPCs after synthesis, toluene solutions of MPCs were drop-coated onto Formvar carbon grids (Electron Microscopy Sciences) prior to imaging (JEOL 1010 TEM). The average diameter of the MPCs was approximately 2.0 (± 0.8) nm and consistent with all of our prior work with these materials.³¹⁻³³ Similarly, 1 μL of formulated sol-gel solutions with and without MPCs were deposited onto grids and allowed to dry overnight prior to imaging. Unless otherwise stated, TEM images were collected at 80 kV; 4,000X magnification.

Cross-sectional TEM to assess the thickness of the MPC-doped sol-gel films was performed as previously demonstrated on MPC film assemblies with some modification.^{33,40} Briefly, a BEEM capsule was filled with EPON resin, inverted on a glass slide and allowed to dry for 48 hours to form a flat epoxy surface. 3 μL of sol-gel solution formulated with MPCs (described above) was then deposited onto the flat surface of the pre-formed resin-filled BEEM capsule and allowed to dry for 48 hours prior at 50% RH. The resin with the MPC-doped sol-gel film was then sliced off and re-embedded in a silicon mold that is then subsequently filled with resin and allowed to dry for 48 hours before being sectioned with a diamond knife (Electron Microscopy Sciences). Thin slices containing a cross-section of the sol-gel film were placed on Formvar-carbon grids (Electron Microscopy Sciences) and imaged using TEM to assess the thickness of the MPC-doped sol-gel film. Unless otherwise stated TEM cross-sectional images were collected at 90 kV; 100,000X magnification.

SEM imaging was performed by drop-casting sol-gel mixtures (3 μL) onto aluminum specimen mounts (Electron Microscopy Sciences) which were allowed to dry for 48 hours in a humidity-controlled environment set to 50% relative humidity (RH). The dried sol-gels films were then sputter-coated with palladium (Denton Desk IV) and subsequently imaged (JEOL 6360 LV SEM).

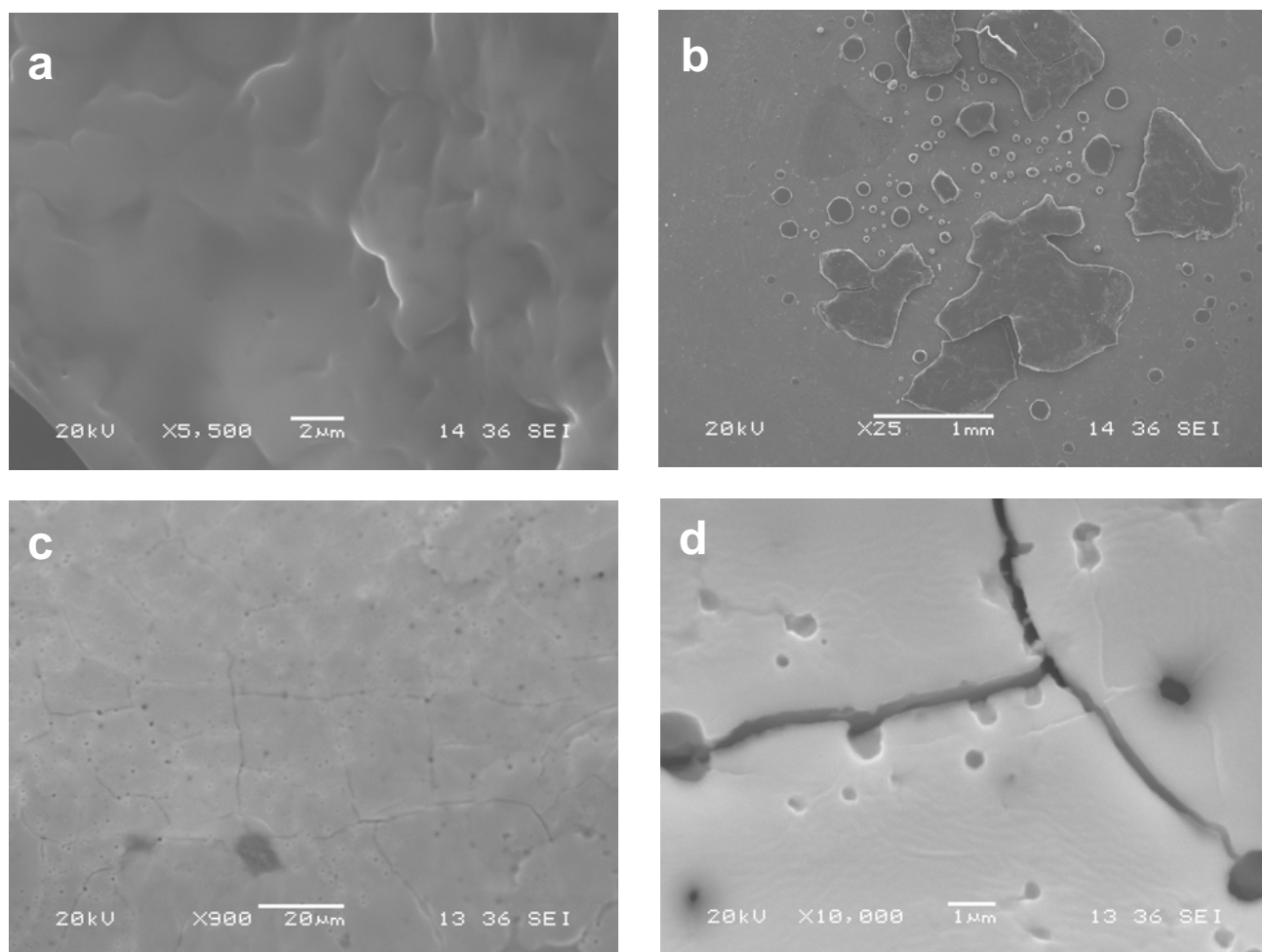


Figure SM-1. SEM imaging of GOx/MPTMS xerogel films (**a,b**) without C6-MPC doping showing lower porosity (deposited and dried for 2 hours at 100% RH before dessicator storage at 0% RH for 48 hours) and (**c,d**) with C6-MPC doping (deposited and dried for 2 hours at 15-20% RH before dessicator storage at 0% RH for 2 hours). Formation and setting of sol-gel films over 2 hours at high relative humidity (100% RH) consistently resulted in films that flaked off the electrode (Supporting Information). Alternatively, films deposited at low humidity (15-20% RH) and then stored continuously at low humidity (0% RH) in a dessicator prior to use showed significant “cracking” under SEM analysis.

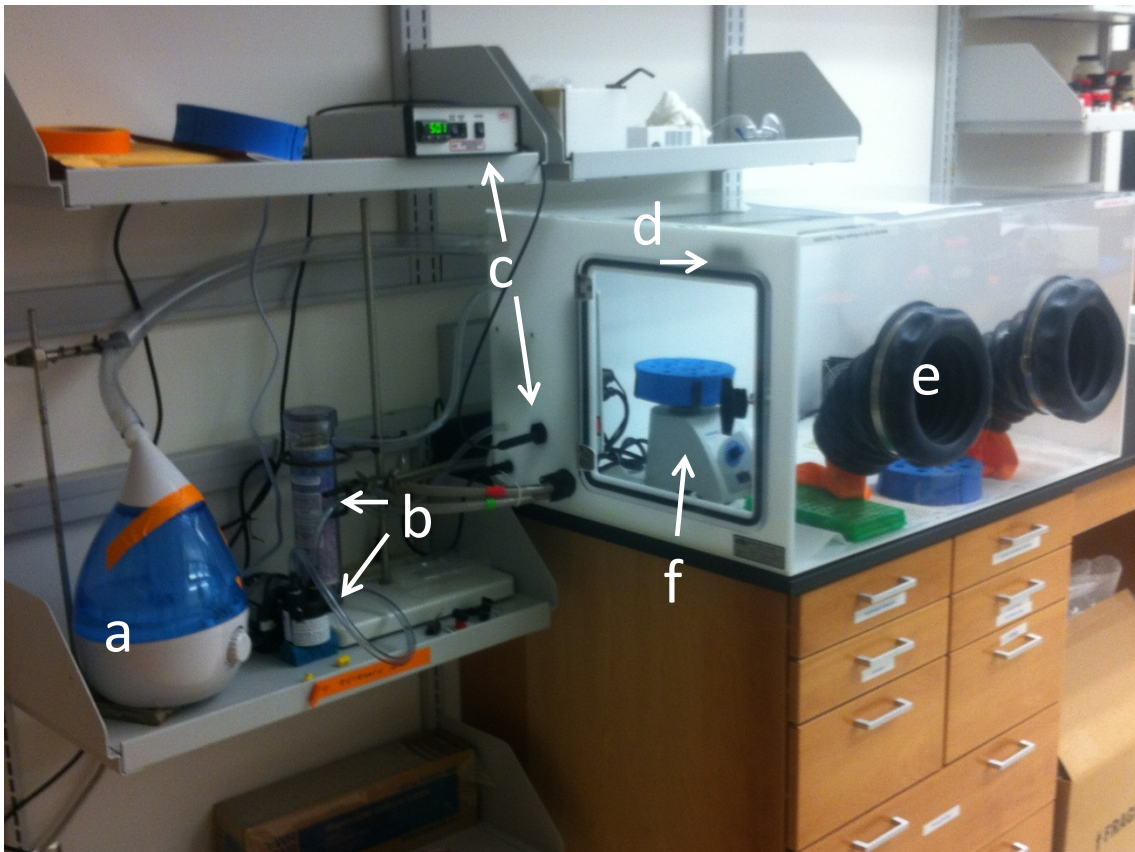


Figure SM-2. Humidity-controlled chamber and apparatus including (a) humidifier; (b) drying column (Dri-Rite) and pump; (c) set-point controller/humidity meter; (d) wireless humidity meter (EasyLog USB); (e) glove box; (f) Vortex.

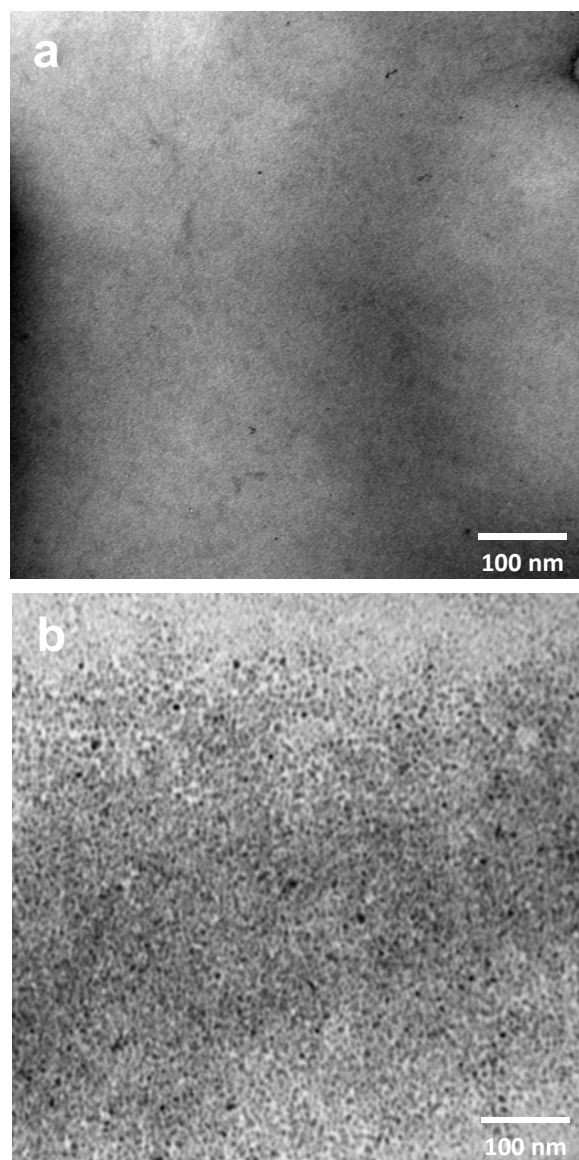


Figure SM-3. Additional examples of TEM imaging of GOx embedded MPTMS xerogel films (a) without and (b) with C6-MPC doping during the sol-gel process.

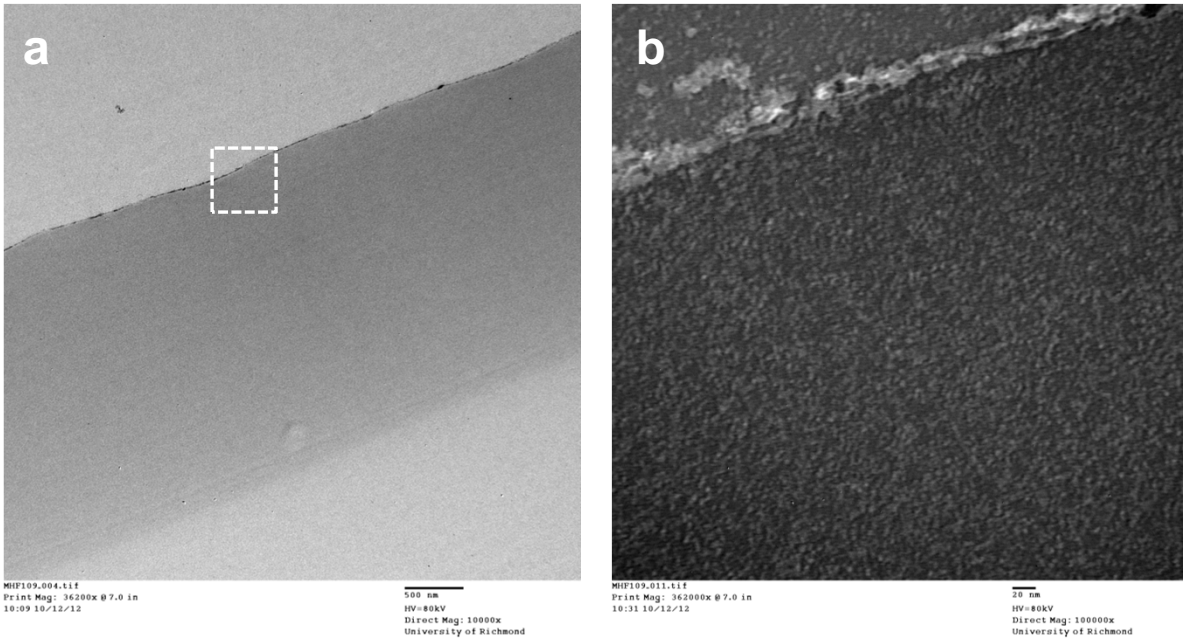


Figure SM-4. TEM cross-sectional imaging of C6-MPC doped MPTMS xerogels (a) with embedded GOx and (b) an expanded image of the designated interface.

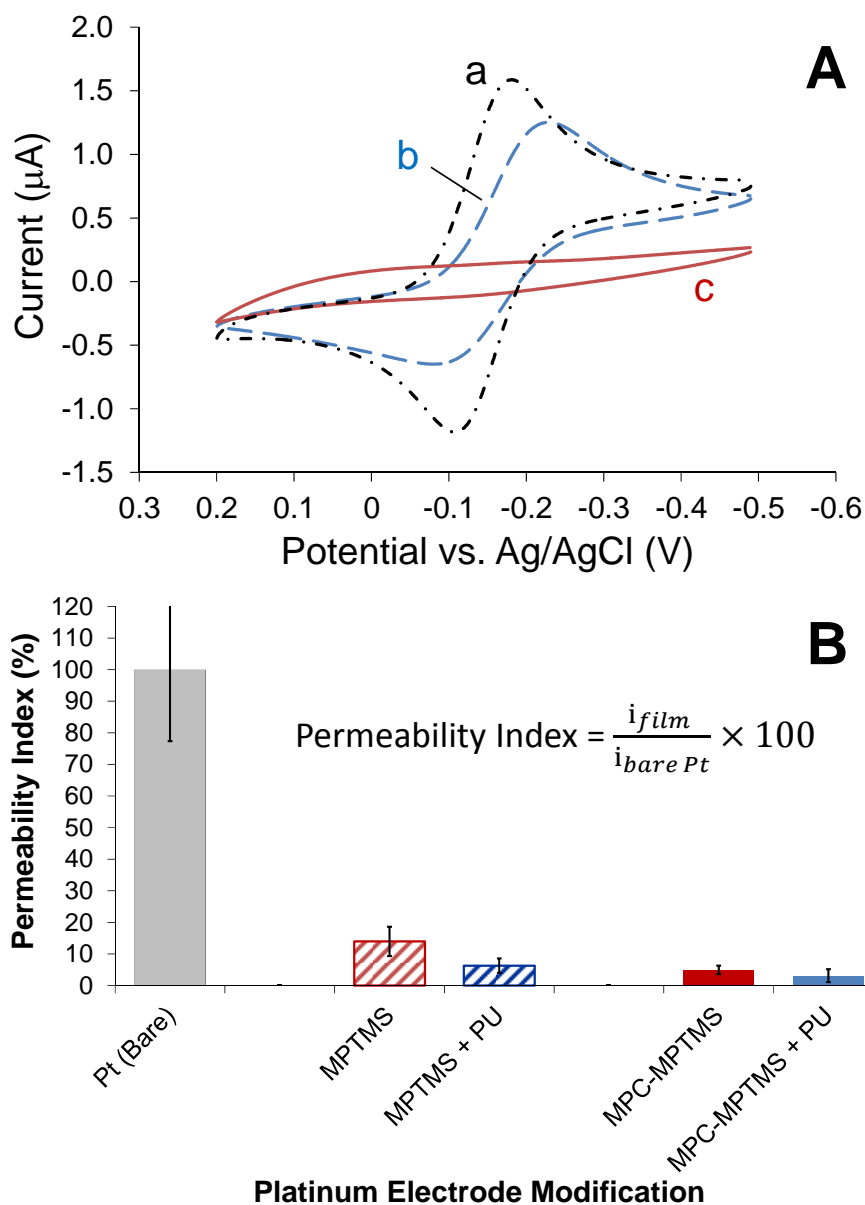


Figure SM-5. (A) Cyclic voltammetry of 2.5 mM ruthenium (III) hexaamine chloride at (a) bare platinum electrode, and modified with GOx embedded 3-MPTMS xerogel films (b) without, and (c) with C6-MPC doping (Note: Similar, completely blocked responses were observed with the addition of PU as well, not shown). Voltammetry was recorded at 100 mV/sec in 0.1 M KNO_3 . (B) Permeability index (%) for 250 μM H_2O_2 for various stages of MPTMS sol-gel films with and without C6-MPC doping and outer polyurethane layer (PU). Permeability index calculated using equation (above) from I-t responses to 10 μL injections of 0.25 M H_2O_2 at an electrode in a stirred solution of 4.4 mM KPB (pH = 7). Xerogels were allowed to dry for 2 hrs. in 15% RH and dessicant dried for 48 hours before analysis.

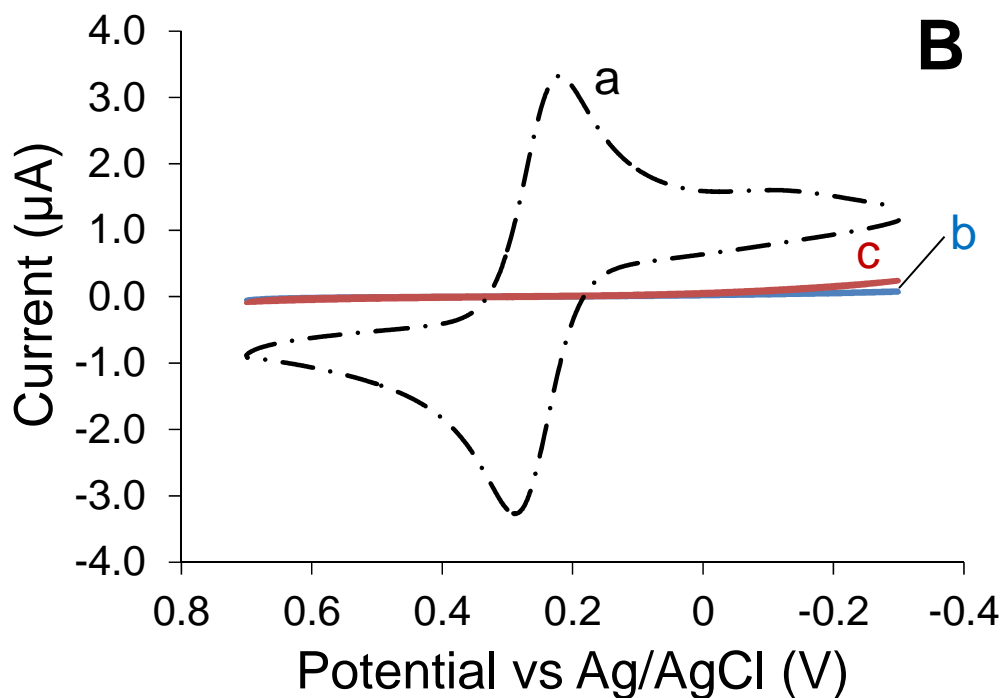
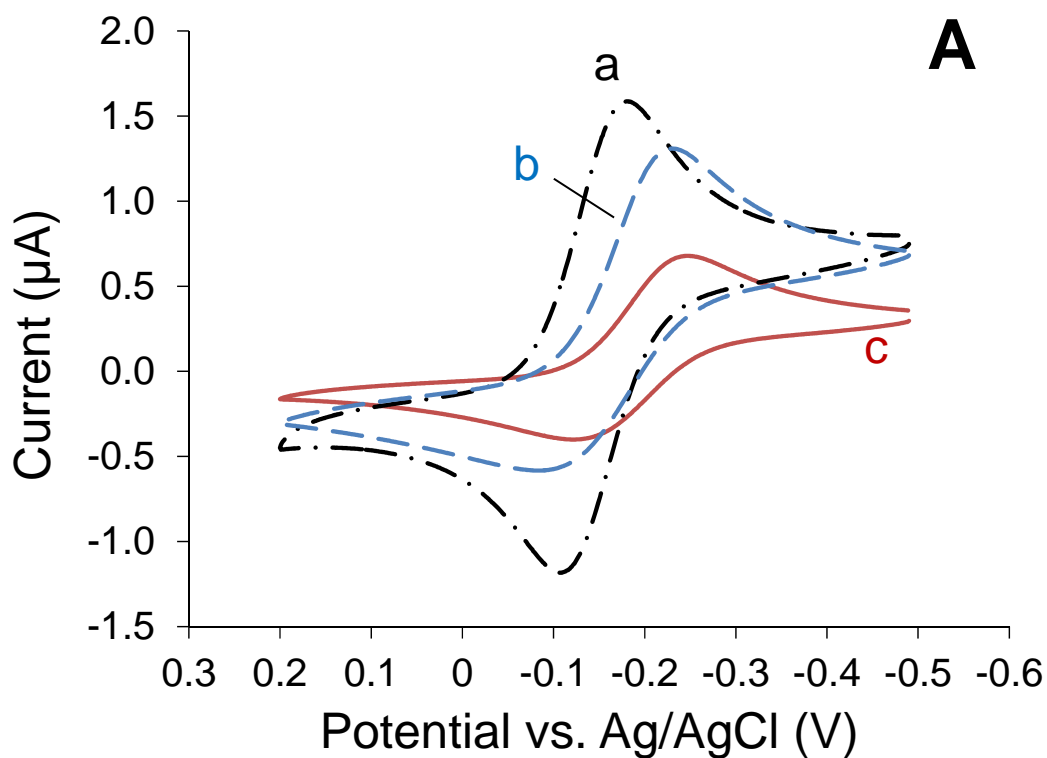


Figure SM-6. Cyclic voltammetry at (a) bare platinum electrode, (b) modified with MPTMS xerogel film, and (c) MPTMS xerogel film doped with C6-MPC for **(A)** 2.5 mM ruthenium (III) hexamine chloride in 0.1 M KNO_3 and **(B)** 5 mM potassium ferricyanide in 0.5 M KCl. Voltammetry was recorded at 100 mV/sec. Xerogels formed over 2 hrs. in 100% RH and dessicant dried for 48 hours before analysis. Results are consistent with Figure 2 and literature.²⁴

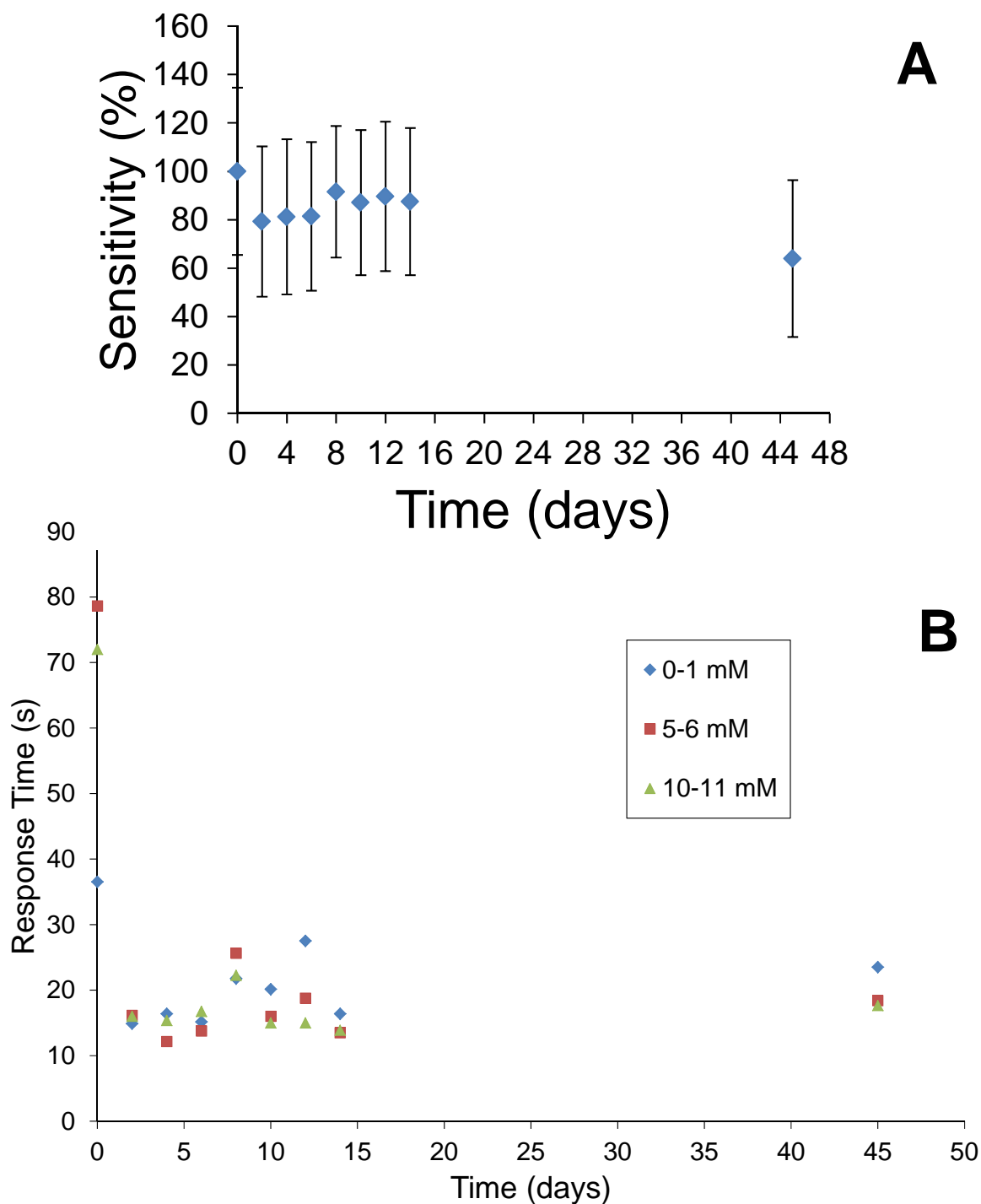


Figure SM-7. Stability tests of MPC-doped glucose sensors over time, including after 45 days, of (A) percent sensitivity (derived from the slope of collected calibration curves) and (B) response time ($t_{r-95\%}$) at 0-1 mM, 5-6 mM, and 10-11 mM glucose injections. After 45 days the sensitivity and response time showed modest degradation, decreasing ~25% and increasing ~35%, respectively.

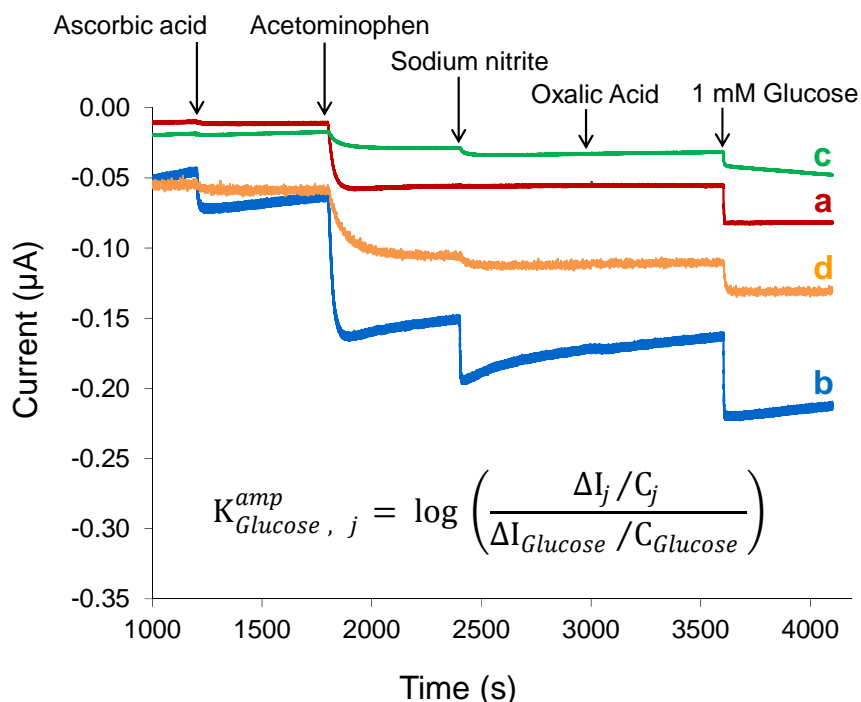


Figure SM-8. Representative amperometric $I-t$ curves during successive injections of interferent species (e.g., ascorbic acid, acetaminophen, sodium nitrite, oxalic acid) and 1 mM glucose at platinum electrodes modified with (a) GOx embedded MPTMS xerogels (un-doped) or GOx embedded MPTMS xerogels doped with (b) C6-MPC, (c) C12 MPC, and (d) MUA-exchanged C6-MPCs and immersed in PBS. All sensors were capped with an outer PU layer. Each injection results in a interferent concentration of 100 μM in the stirred 4.4 mM PBS (pH=7) . Xerogels were allowed to dry over 48 hrs. in 50% controlled RH before analysis. **Inset:** Selectivity coefficient (K) where ΔI_j and $\Delta I_{\text{glucose}}$ are the measured currents for a specific interferent species (j) and glucose at concentrations of C_j and C_{glucose} , respectively. We note that the enhanced glucose signal observed with the incorporation of the MPCs into the sol-gel can also result, in some cases, in a corresponding enhancement of the interferent signal as well, a phenomenon explored further when the function of the MPCs within the sensing scheme mechanism are examined in detail.

Table 1: Selectivity Coefficients of Interferents at PU Coated GOx/MPTMS Sensors

Interferent Species (100 μM)	MPTMS sol-gel	C6 MPC-doped	C12 MPC-doped	C6/MUA MPC-doped
Ascorbic acid	-0.47(± 0.15)	0.39(± 0.15)	-0.06(± 0.12)	0.24(± 0.12)
Acetaminophen	0.64(± 0.20)	0.89(± 0.14)	0.61(± 0.21)	1.2(± 0.047)
Sodium nitrite	NR	0.04(± 0.44)	0.55(± 0.18)	0.53(± 0.18)
Oxalic acid	NR	NR	NR	NR
Uric acid ^a	NR	NR	NR	NR

Notes: All interferent injections resulted in a 100 μM concentration in stirred 4.4 mM PBS (pH=7); ^auric acid had a bulk concentration of 300 μM at the sensor interface. "NR" indicates that there was no amperometric response for that particular interferent at the described interface.

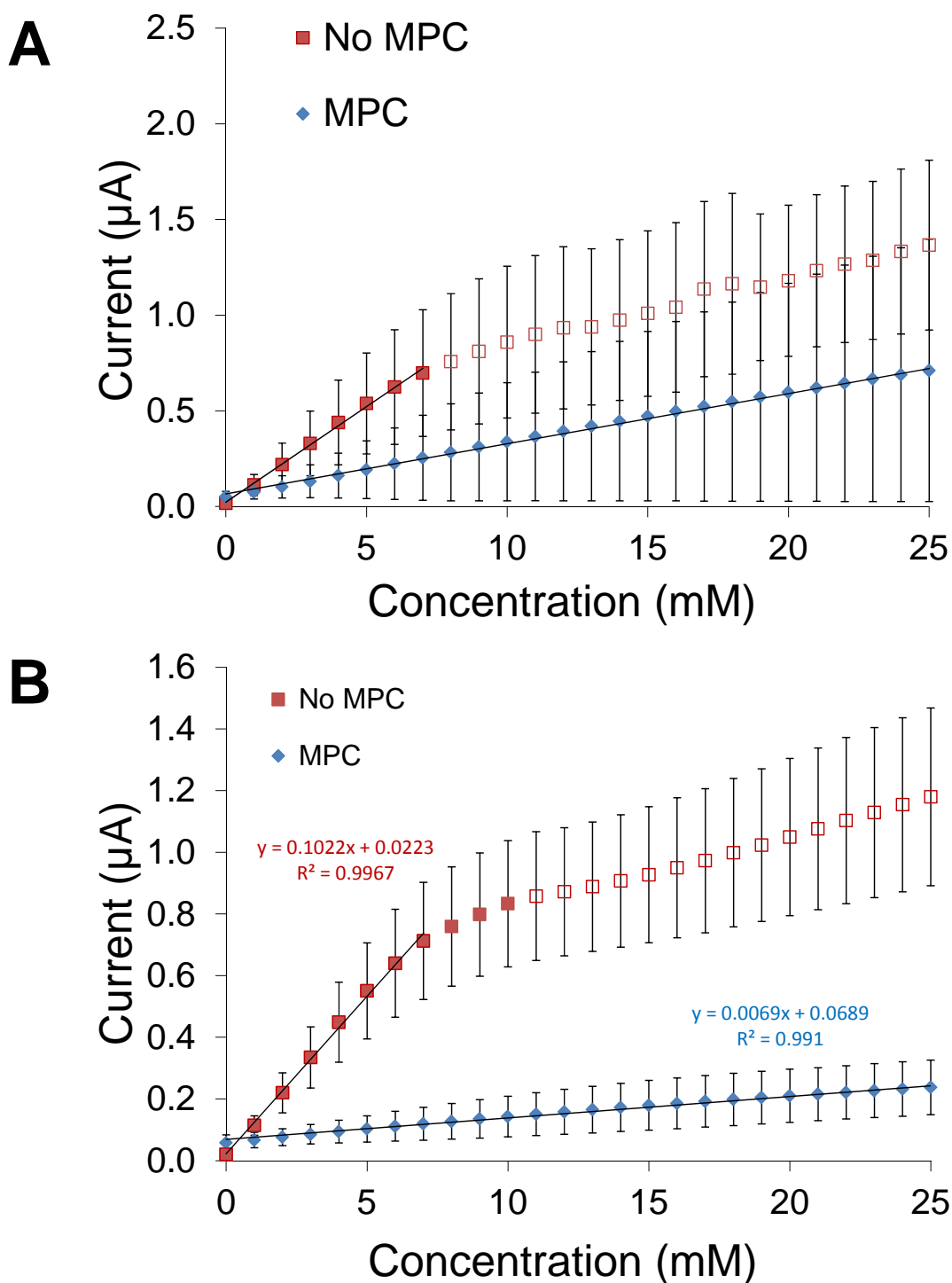


Figure SM-9. Calibration curves showing the linear range for glucose biosensors with GOx embedded MPTMS xerogels with and without C6-MPC doping formed and tested (A) with variable drying time (30 minutes to 48 hours) and humidity control or (B) with a controlled 30 minute drying time at 50% controlled relative humidity. Note: Solid symbols ($\blacklozenge, \blacksquare$) indicate a step-like response to glucose concentration increases whereas open symbols (\diamond, \square) indicate a non-step response (dynamic range).

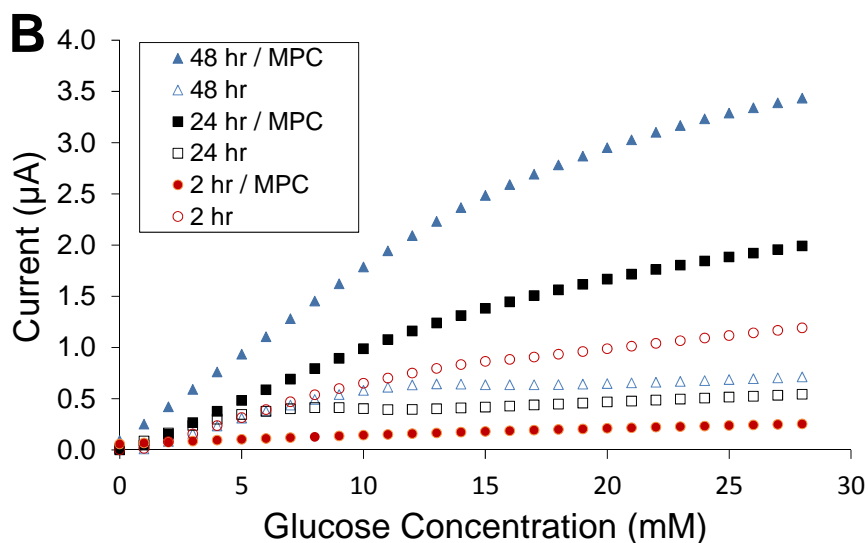
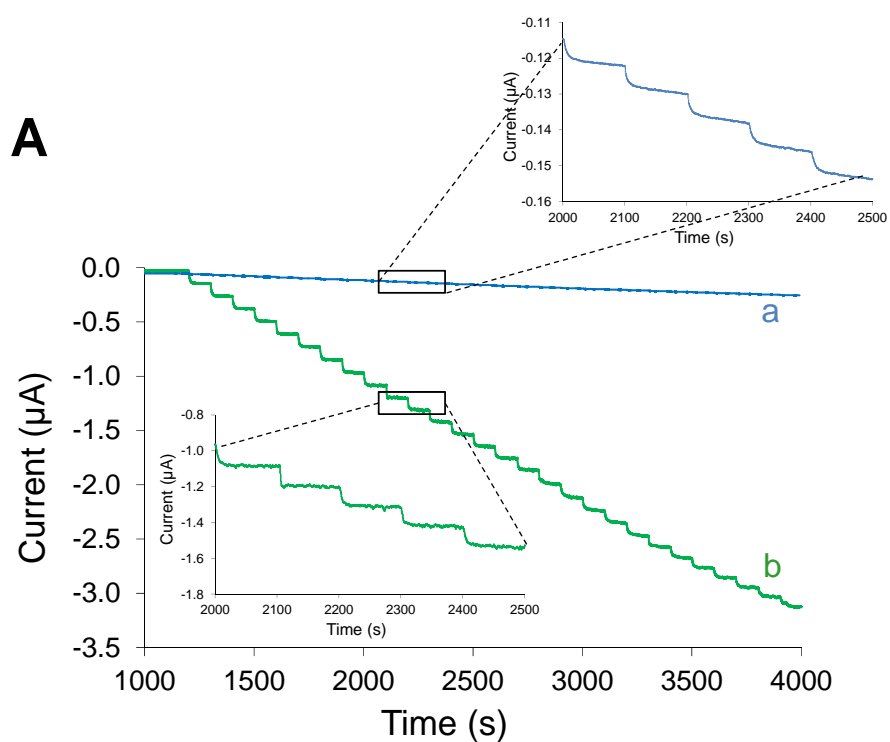


Figure SM-10. (A) Representative amperometric $I-t$ curves during successive injections of glucose at MPC-doped MPTMS xerogels embedded with GOx and coated with with PU where the gel was allowed to dry under 50% RH for (a) 2 hours or (b) 48 hours. Each 10 μL injection (1.0 M glucose) at every 100 second interval results in a 1 mM glucose increase of the stirred 4.4 mM PBS (pH=7); (B) Calibration curves of GOx/MPTMS xerogel sensors formed with (*solid symbols*; \blacktriangle , \blacksquare , \bullet) and without (*open symbols*; \triangle , \square , \circ) C6-MPC doping and dried for 2, 24, and 48 hours in controlled 50% relative humidity. Note: Uncertainty (error bars) not shown for clarity.

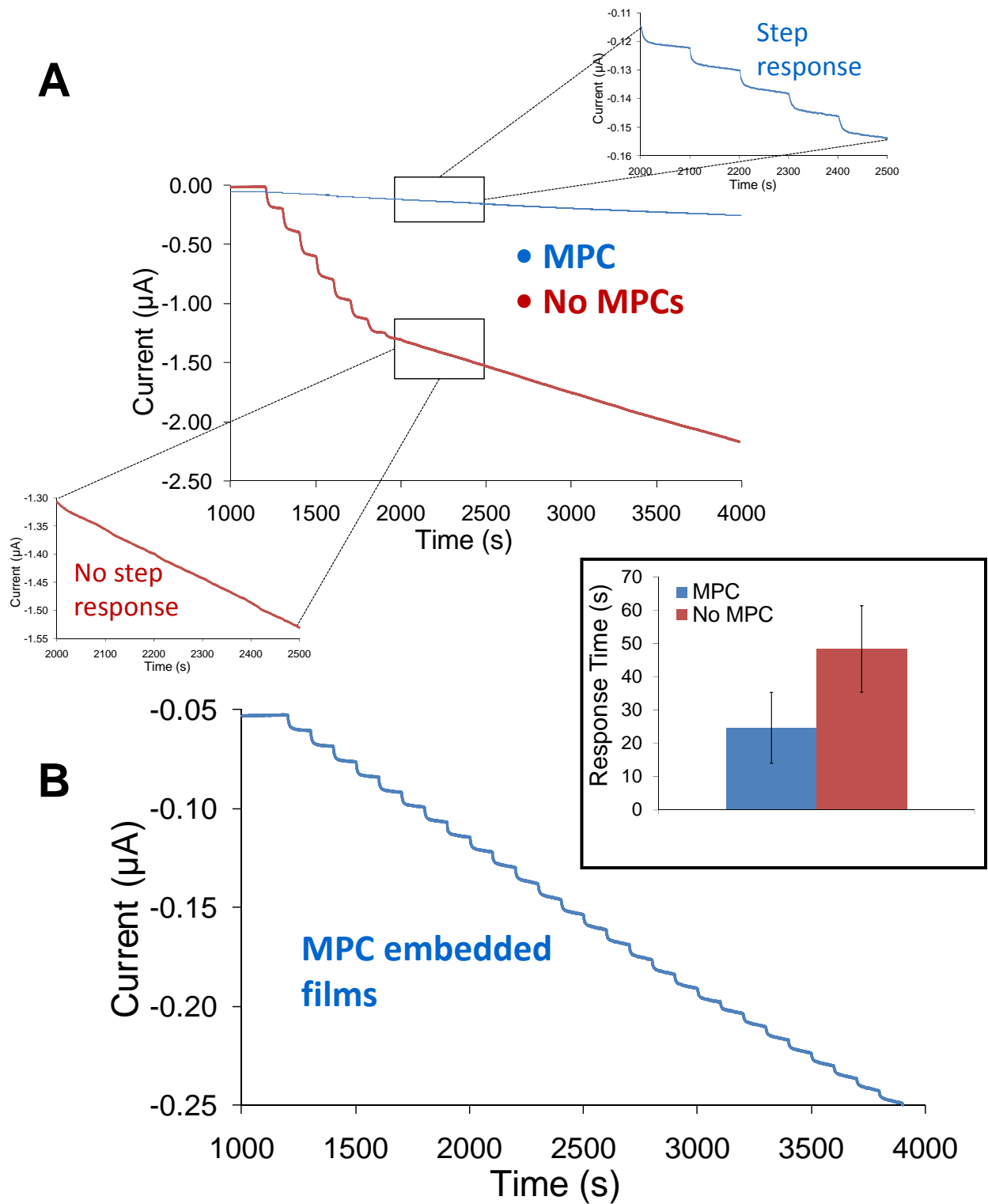


Figure SM-11. (A) Representative amperometric $I-t$ curves during successive injections of glucose at platinum electrodes modified with (a) GOx embedded MPTMS xerogel and (b) GOx embedded MPTMS xerogel doped with C6-MPCs. Each 10 μL injection (1.0 M glucose) at every 100 second interval results in a 1 mM glucose increase of the stirred 4.4 mM PBS (pH=7). (B) Expansion of typical “low current” $I-t$ curve for GOx/MPTMS xerogels doped with C6-MPCs that yield smaller current step responses over a larger linear range and with greater response time (inset) compared to films without embedded NPs. Xerogels allowed to dry for 2 hrs. in 50-60% RH before analysis.

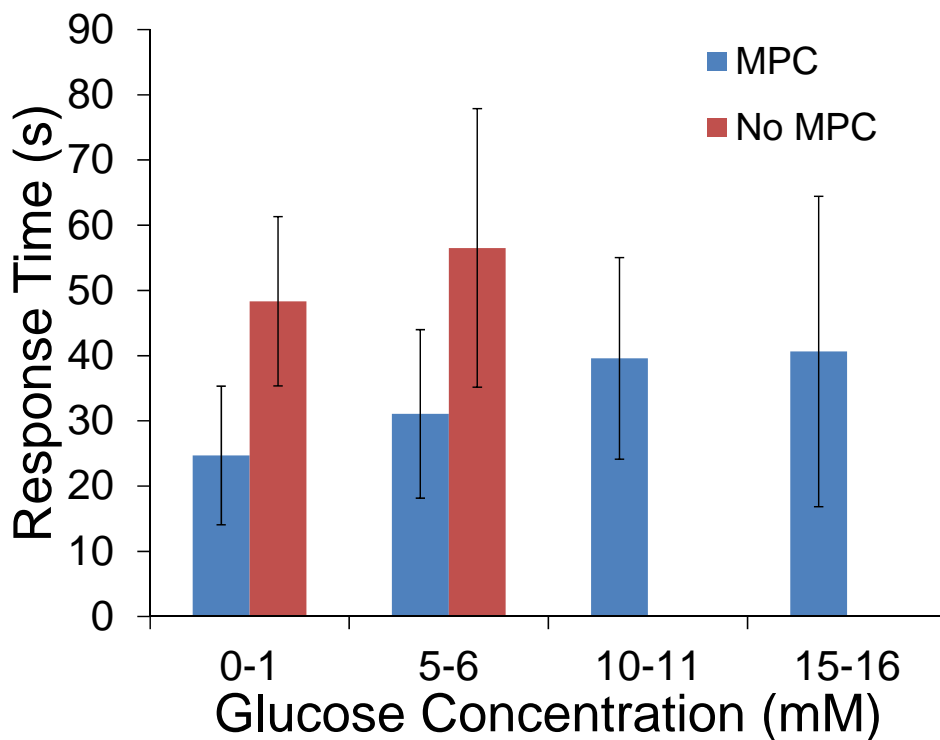


Figure SM-12. Glucose response time ($t_{r,95\%}$) comparison for increasing concentrations of glucose for sensors with and without C6-MPC doping for films performing in the low current response regime (i.e., xerogels allowed to dry for 2 hrs. in 50-60% RH before analysis). We note that the improvement in response time becomes less significant at higher glucose concentrations compared to films allowed to dry for 48 hours (Figure 6).

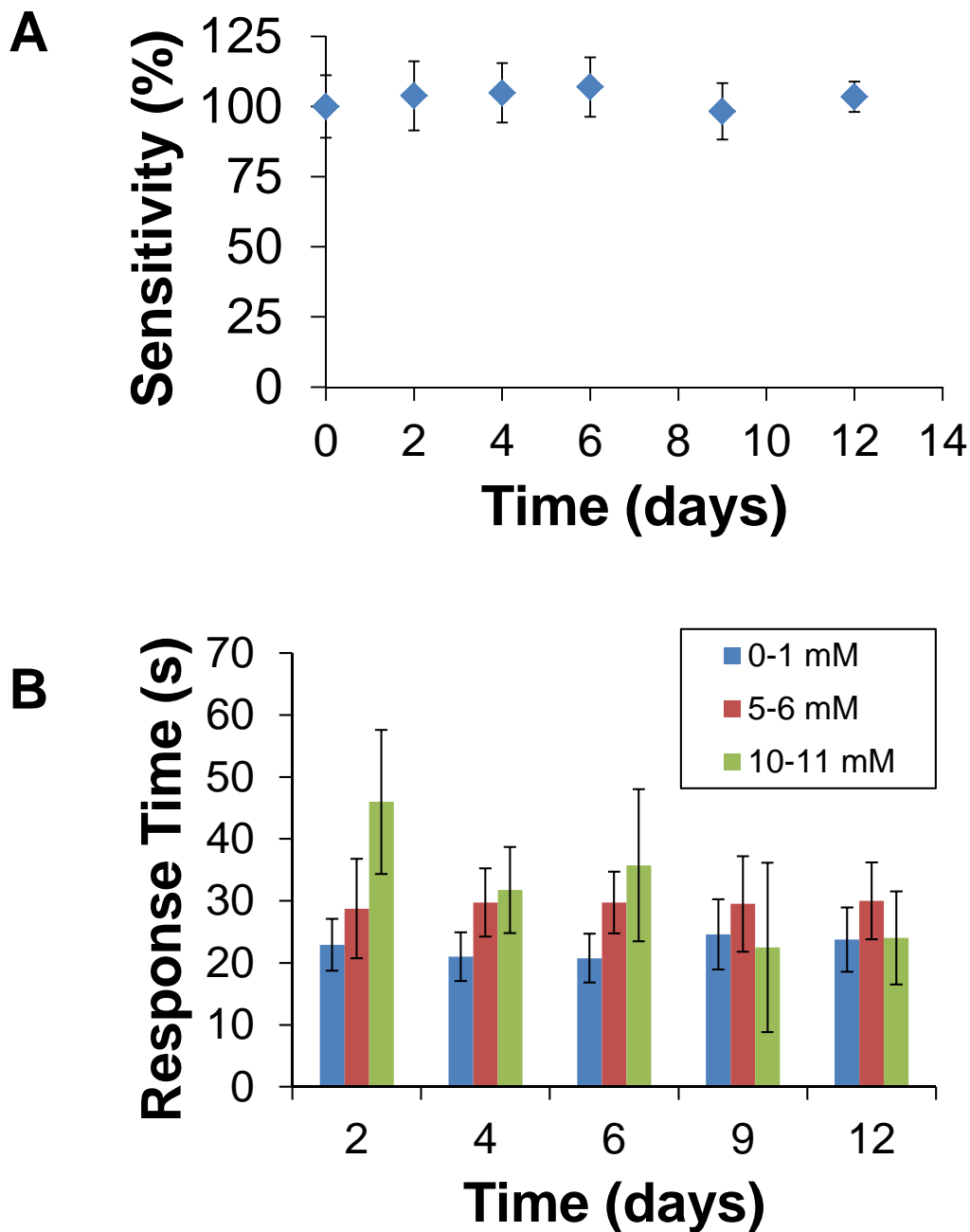


Figure SM-13. Stability tests of the “low current” regime MPC-doped glucose sensors, monitored over two weeks for (A) percent sensitivity (derived from the slope of collected calibration curves) and (B) percent response time ($t_{r-95\%}$) at 0-1 mM, 5-6 mM, and 10-11 mM glucose injections.

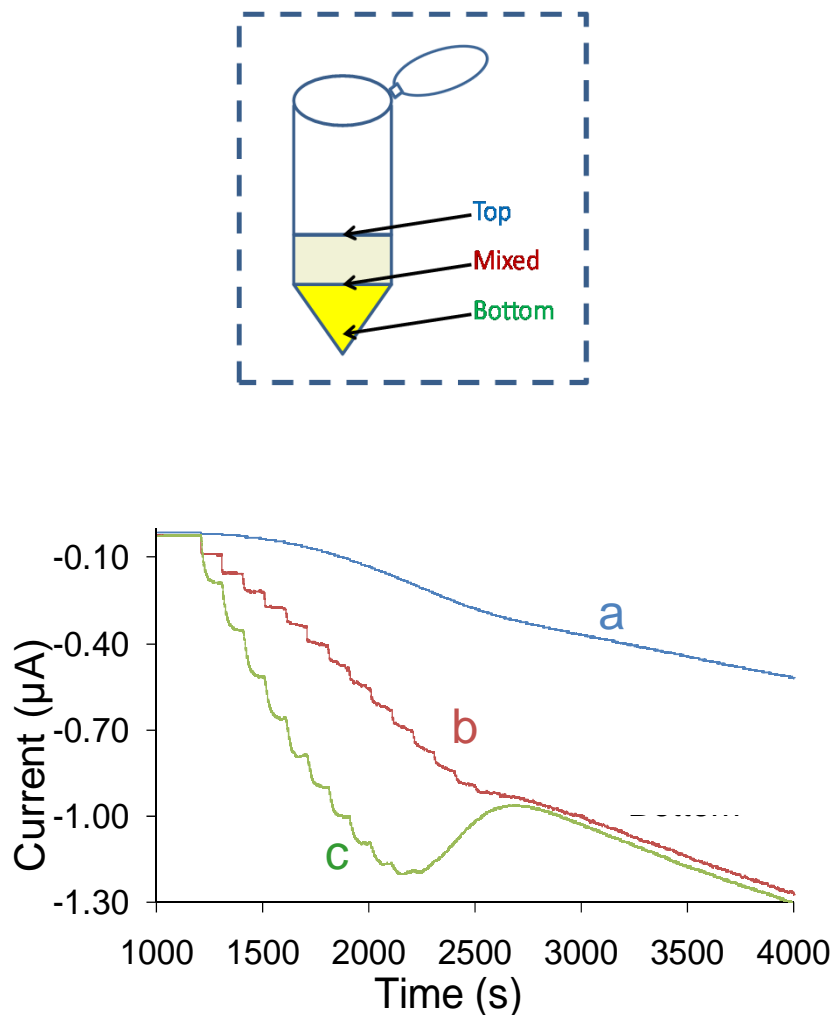


Figure SM-14. Representative $I-t$ curves for GOx embedded MPTMS xerogels doped with C6-MPCs where the sol-gel deposition mixture was drawn either from the (a) top, (b) middle, or (c) bottom of the mixing vial, a parameter affecting the magnitude of current response and range of “step” response to glucose. Sampling from the bottom of the mixture initiates higher water-to-silane ratios that result in more porous sol-gels which allow greater glucose permeability and higher current signals. Sampling from the top of the mixture creates the opposite effect and gives rise to the low and high current regimes observed with these sensors.

Table SM-1: Comparison of amperometric glucose biosensor performance with and without nanomaterials

System	WE	Linear Range ^a (mM)	Dynamic Range ^a (mM)	Sensitivity (μA/mM)	Response Time (s)	LOD, 3σ _{BL} (μM) ^b	Stability	Ref ^c
MPTMS	Pt	7	12	0.072 _(0.002)	45.5 _(25.9) ^e	30.7 _(20.4)	>2 wk.	<i>d.</i>
MPTMS with MPCs	Pt	14	22	0.184 _(0.005)	11.3 _(6.6) ^e	23.2 _(5.5)	>2 wk.	<i>d.</i>
Sol-gel Based Glucose Sensors (without NPs)								
MPTMS	Pt	12.5	20	0.0035	11-12 ^e	-	5 mo.	<i>1</i>
TEOS	ITO	15	30	-	<30	-	2 mo.	<i>2</i>
MTMOS	Pt	20-30	-	0.038	20-65 ^e	-	2 wk.	<i>3</i>
MTMOS	Pt	-	6	0.11	28.2 ^e	-	-	<i>4</i>
MPTMS/TEOS	GCE	4.4	-	0.81	15 ^f	19	3 wk.	<i>5</i>
Nafion (Wire)	Pt	9	20	0.0022	60 ^e	-	2 wk.	<i>6</i>
Glucose Sensors (with NPs)								
MPTMS sol-gel/CSNPs	Au	6	-	0.26	3 ^e	23	2 mo.	<i>7</i>
Cysteamine films/CSNPs	Au	8	-	0.18	4	8	4 wk.	<i>8</i>
CSNPs/ CNT	Au	9	-	0.23	-	128	3 wk.	<i>9</i>
APTES sol-gel/AuNPs (3 rd G)	GCE	.05	.120	0.027	-	0.1	2 wk.	<i>10</i>
MPTMS/AuNPs (2 nd G)	Au	5E-5	5E-5	13.8	-	-	3 wk.	<i>11</i>
TEOS, CSNP, (2 nd G)	GrP	55	-	2.43	-	1300	3-4 wk	<i>12</i>
PVC/TFP-TCNQ	-	2	-	4.5E4	-	6.2	-	<i>13</i>
MPTMS sol-gel/CSNPs (lactate)	Au	0.6	0.9	0.45	2-3	0.1	-	<i>14</i>
MPTMS sol-gel/CSNPs (3 rd G)	Au	8	12	3.6E-6	-	.05	24 hr.	<i>15</i>
CSNPs & Silica NPs	Pt	<10	30	-	60	-	-	<i>16</i>

(a) Upper limit of range listed; (b) Limit of Detection (L.O.D.) is the concentration required to elicit a sensor response (3σ_{BL}); (c) References listed below; (d) This work compares a first-generation glucose oxidase-based amperometric biosensor with MPCs to one without;

Response times calculated with (e) 95% maximum response or (f) 90% maximum response (all others were unspecified).

Notes:

CS-NPs: Citrate-stabilized colloidal gold nanoparticles; MPTMS: 3-mercaptopropyltrimethoxy silane; MTMOS: methyltrimethoxy silane; TEOS: tetraethoxy silane; TMOS: tetramethoxy silane; APTEOS: 3-aminopropyltriethoxy silane; CNTs: carbon nanotubes; 3rd G: Third-generation reagentless biosensor; 2nd G: Employs an electron transfer mediator; GrP: Graphite powder

References – Table SM-1

1. Yang, Y.; Tseng, T.; Yeh, J.; Chen, C.; Lou, S. *Sensors and Actuators B*. **2008**, 131, 533-540.
2. Narang, U.; Prasad, P. N.; Bright, F. V. *Anal. Chem.* **1994**, 66, 3139-3144.
3. Shin, J. H.; Marxer, S. M.; Schoenfisch, M. H. *Anal. Chem.* **2004**, 76, 4543-4549.
4. Koh, A.; Riccio, D. A.; Sun, B.; Carpenter, A. W.; Nichols, S. P.; Schoenfisch, M. H. *Biosens. and Bioelectron.* **2011**, 28, 17-24.
5. Liu, S.; Sun, Y. *Biosensors and Bioelectronics.* **2007**, 22, 905-911.
6. Ward, W. K.; Jansen, L. B.; Anderson, E.; Reach, G.; Klein, J. C.; Wilson, G. S. *Biosensors and Bioelectronics.* **2002**, 17, 181-189.
7. Zhang, S.; Wang, N.; Niu, Y.; Sun, C. *Sensors and Actuators B*. **2005**, 109, 367-374.
8. Yang, W.; Wang, J.; Zhao, S.; Sun, Y.; Sun, C. *Electrochem. Commun.* **2006**, 8, 665-672.
9. Liu, Y.; Wu, S.; Ju, H.; Xu, L. *Electroanalysis.* **2007**, 19, 986-992.
10. Zhang, J.; Zhu, J. *Science in China, Series B: Chemistry.* **2009**, 52, 815-820.
11. Zhong, X.; Yuan, R.; Chai, Y.; Liu, Y.; Dai, J.; Tang, D. *Sensors and Actuators B*. **2005**, 104, 191-198.
12. Barbadillo, M.; Casero, E.; Petit-Domínguez, M.; Vásquez, L.; Pariente, F.; Lorenzo, E. *Talanta.* **2009**, 80, 797-802.
13. Sánchez-Obrero, G.; Cano, M.; Ávila, J.; Mayén, M.; Mena, M.; Pingarrón, J.; Rodríguez-Amaro, R. *Journal of Electroanalytical Chemistry.* **2009**, 634, 59-63.
14. Jena, B.; Raj, C. *Anal. Chem.* **2006**, 78, 6332-6339.
15. Jena, B.; Raj, C. *Chem. Eur. J.* **2006**, 12, 2702-2708.
16. Tang, F.; Meng, X.; Chen, D.; Ran, J.; Zheng, C. *Science in China, Series B: Chemistry.* **2000**, 43, 268-274.